JOURNAL OF GUIDANCE, CONTROL, AND DYNAMICS
Vol. 16, No. 6, November–December 1993

Input-Shaped Control of Three-Dimensional Maneuvers of Flexible Spacecraft

T. Singh* and S. R. Vadali†
Texas A&M University, College Station, Texas 77843

This paper deals with the control of three-dimensional rotational maneuvers of flexible spacecraft. A spacecraft model with a cylindrical huh and four symmetric appendages is considered. The appendages are tong and flexible, leading to low-frequency vibration under any control action. To provide a comprehensive treatment of input-shaped controllers (time-delay filters), both open-loop and closed-loop maneuvers are considered. For the open-loop maneuver, a five-switch, near-minimum-time bang-bang controller is designed based on the rigid-body model. The design procedure accounts for the presence of the time-delay filter for determining the switch times. In addition, a combination of a Lyapunov controller with the time-delay control technique is proposed to take advantage of the simple feedback control strategy and augment it with a technique that can eliminate the vibratory motion of the flexible appendages more efficiently.

I. Introduction

IN this paper the problem of reorientation of a hub-appendage structure is considered. Considerable work has been done on Lyapunov control of single-axis maneuvers of hub-appendage structures.[1-4] Hablani[5] provides a technique for the estimation of the switch times for a bang-bang profile for zero residual energy, single-axis slew of a flexible spacecraft. Techniques are provided to estimate switch times for a system with either damped or undamped modes. A weighted time-fuel optimal controller for the rest-to-rest slew with zero residual energy is designed using the principles of dynamics by Skaar et al.[6] An elegant input-shaping scheme proposed by Smith[7] and later modified by Singer and Seering[8] has been used by Wie and Liu[9] to modify the flexible-body time optimal control profile to produce a robust control scheme, which has been applied to the control of a two-mass spring model.

Here we consider the three-dimensional case, leading to a model that has kinematic and dynamic nonlinearities. The system under consideration consists of a cylindrical hub, with four cantilevered cylindrical appendages of equal dimensions (Fig. 1). In modeling this system, only those modes that will be excited by a hub torque are considered. These modes lead to displacements of the appendages (which are modeled as Euler-Bernoulli beams), which resemble a three-dimensional starfish. The equations of motion of the flexible appendages are arrived at using the Lagrangian approach, and the rigid-body equations are arrived at using the Newton-Euler technique. The assumed modes technique is used to transform the partial differential equations (representing the equations of motion of the flexible appendages) to ordinary differential equations. Two modes are used to represent the displacement of each of the flexible appendages in the simulation of the system.

The first controller proposed in this study is based on the amalgamation of two powerful control techniques. First, the rigid-body controller is designed based on the Lyapunov stability concept, which leads to a simple control law that involves feeding back the Euler parameters and the angular velocities of the system. With this feedback controller in place, a time-delay controller is designed based on the eigenvalues of the system linearized about the final position. The benefit of using this combination is made evident by the reduction in the deflection of the appendages and the maximum applied torque. The second controller utilizes a bang-bang profile designed for the rigid body, which has a time-delay prefilter associated with it. A comparison of various controllers mentioned previously is provided in the penultimate section of this paper.

11. Modeling

The derivation of the equations of motion is carried out symbolically using Mathematica. The radius of the hub is a (Fig. 2) and the appendages are of length L. The radius vector of points on the two appendages in the body fixed frame are

$$\underline{r}_1 = \begin{Bmatrix} (a+\xi) \\ y_1 \\ y_2 \end{Bmatrix} \tag{1}$$

for the first appendage and

$$\underline{r}_2 = \begin{Bmatrix} -y_1 \\ (a+\xi) \\ y_3 \end{Bmatrix} \tag{2}$$

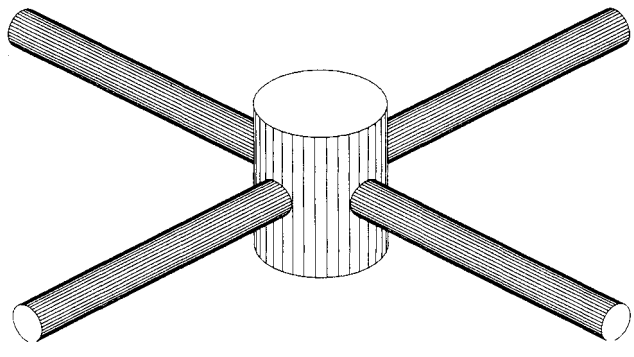

Fig. 1 Schematic of the hub-appendage spacecraft.

Received Nov. 14, 1991; revision received Dec. 1, 1992; accepted for publication Dec. 28, 1992.

*Post Doctoral Fellow, Department of Aerospace Engineering; currently Assistant Professor, Department of Mechanical and Aerospace Engineering, State University of New York at Buffalo, Buffalo, NY. Member AIAA.

†Associate Professor, Department of Aerospace Engineering. Associate Fellow AIAA.

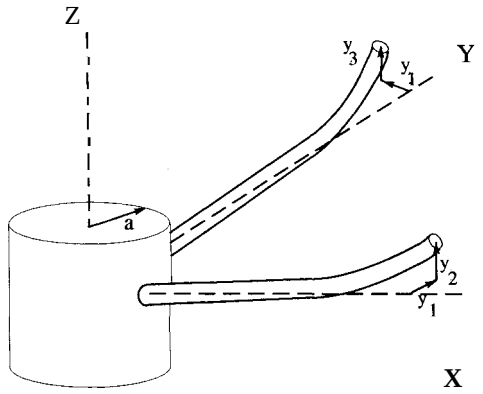

Fig. 2 Flexible spacecraft configuration.

for the second appendage. Here ξ is the independent variable indicating position on the appendage. It is assumed that the flexible appendages deform in a starfish fashion, leading to the deformation of the first appendage in the y direction being the negative of the deformation of the second appendage in the X direction.

The deformation of the appendages can be represented as

$$y_i = \sum_{j=1}^{m} \phi_{ij}(\xi) q_{ij}(t) \tag{3}$$

where m is the number of assumed modes. The assumed modes[10] chosen for this model are

$$\phi_{ij}(\xi) = 1 - \cos(j\pi\xi/L) + \%(-1)^{j+1}(j\pi\xi/L)^2 \qquad j = 1 \text{ to } 2 \tag{4}$$

The Euler-Lagrange equations of motion for the flexible modes are arrived at after determining the potential and kinetic energy of the system. The potential energy is represented as

$$V = \left\{ \frac{1}{2} \int_0^L EI[2(y_1'')^2 + (y_2'')^2 + (y_3'')^2] \, \mathrm{d}\xi \right\} \tag{5}$$

where EI is the flexural rigidity of the appendage and $(\,)''$ represents the second spatial derivative. The kinetic energy is

$$T = \frac{1}{2} \underline{\omega}^T I_{\text{hub}} \underline{\omega} + 2\left[\frac{1}{2} \sum_{i=1}^{2} \int_0^L \underline{\dot{r}}_i^T \underline{\dot{r}}_i \rho A \, \mathrm{d}\xi \right] \tag{6}$$

where I_{hub} is the mass moment of inertia of the hub, ρA is the mass density per unit length, and $\underline{\omega}$ is the angular velocity vector

$$\underline{\omega} = \begin{Bmatrix} \omega_1 \\ \omega_2 \\ \omega_3 \end{Bmatrix} \tag{7}$$

with components in the body-fixed frame.

The Euler-Lagrange equations of motion for the flexible modes are

$$\frac{\mathrm{d}}{\mathrm{d}t} \frac{\partial L}{\partial \dot{q}_{ij}} - \frac{\partial L}{\partial q_{ij}} = 0 \tag{8}$$

where q_{ij} are the generalized coordinates and L $= T -$ V is the Lagrangian of the system.

The rigid-body equations of motion are arrived at from the angular momentum of the system, which is

$$= 2 \sum_{i=1}^{2} \int_0^L \underline{r}_i \times \underline{\dot{r}}_i \rho A \, \mathrm{d}\xi + I_{\text{hub}} \underline{\omega} \tag{9}$$

The derivative of the angular momentum is

$$\dot{\underline{H}} = \dot{\underline{H}}_b + \underline{\omega} \times \underline{H} = \underline{U} \tag{10}$$

where the subscript b refers to the body-fixed frame and $\underline{U}$ is the torque vector. In the interest of brevity the equations of motion are not included here.

III. Closed-Loop Control: Lyapunov Controller

The Lyapunov control design process starts with a choice of a candidate Lyapunov function, which for the present system is a combination of the kinetic, flexural, and pseudopotential energies. The choice here is a generalization to the three-dimensional space of the single-axis Lyapunov function.[1] The Euler parameter differential equations are

$$\underline{\dot{\beta}} = \tfrac{1}{2} G(\beta) \underline{\omega} \tag{11}$$

where

$$G(\beta) = \begin{vmatrix} -\beta_1 & -\beta_2 & -P3 \\ P0 & -\beta_3 & \beta_2 \\ P3 & P0 & -\beta_1 \\ -\beta_2 & \beta_1 & P0 \end{vmatrix} \tag{12}$$

At time $t = 0$,

$$\underline{\beta} = \underline{\beta}(0) \tag{13}$$

The desired equilibrium is

$$\underline{\beta} = \underline{\beta}_f \tag{14}$$

and $\underline{\beta}_f$ is not necessarily [1 0 0 0]. Then the error quaternion at any instant is

$$\begin{bmatrix} \beta_{0_e} \\ \beta_{1_e} \\ \beta_{2_e} \\ \beta_{3_e} \end{bmatrix} = \begin{bmatrix} \beta_{0_f} & \beta_{1_f} & \beta_{2_f} & \beta_{3_f} \\ -\beta_{1_f} & \beta_{0_f} & \beta_{3_f} & -\beta_{2_f} \\ -\beta_{2_f} & -\beta_{3_f} & P0, & \beta_{1_f} \\ -\beta_{3_f} & \beta_{2_f} & -\beta_{1_f} & P0, \end{bmatrix} \begin{vmatrix} \beta_0 \\ \beta_1 \\ \beta_2 \\ \beta_3 \end{vmatrix} \tag{15}$$

We define a pseudopotential energy function

$$\Phi = (\beta_{0_e} - 1)^2 + \beta_{1_e}^2 + \beta_{2_e}^2 + \beta_{3_e}^2 \tag{16}$$

We can show that

$$= 2(\beta_{0_e} - 1)\dot{\beta}_{0_e} + 2\beta_{i_e}\dot{\beta}_{i_e} = -2\dot{\beta}_{0_e} \tag{17}$$

$$\Rightarrow -[\beta_{0_f} \ \beta_{1_f} \ \beta_{2_f} \ \beta_{3_f}] G(\beta) \underline{\omega} = \tilde{\underline{\beta}}_e^T \underline{\omega} \tag{18}$$

where $\tilde{\underline{\beta}}_e$ is the reduced error quaternion

$$\tilde{\underline{\beta}}_e = [\beta_{1_e} \ \beta_{2_e} \ \beta_{3_e}]^T \tag{19}$$

Let the Lyapunov function be

$$V = T + V + k_1 \Phi = E + k_1 \Phi \tag{20}$$

where k_1 is a positive definite scalar. Other forms of the Lyapunov function can be found in Ref. 11. The rate of change of E can be evaluated using the work-energy rate principle[12]:

$$\dot{E} = \underline{\omega}^T \underline{U} \tag{21}$$

Therefore

$$\dot{V} = \underline{\omega}^T [\underline{U} + k_1 \tilde{\underline{\beta}}_e] \tag{22}$$

The feedback control law that renders the closed-loop system asymptotically stable is given by

$$\underline{U} = -k_1\tilde{\beta}_e - K_2\underline{\omega} \tag{23}$$

where K_2 is a positive definite gain matrix. For simplicity, K_2 was chosen as a diagonal matrix with the gain for each axis being k_2. The specific numerical choice of the gains was made using a model obtained by linearizing the system about the desired final state. For this purpose, the following relations were utilized:

$$\omega_i = 8; \tag{24}$$

$$\beta_{e_i} = \theta_i/2 \qquad i = 1, 2, 3 \tag{25}$$

where θ_i are the Euler angles. The linearized rigid-body equations are

$$I_{Ti}\dot{\omega}_i = u_i \qquad \text{i} = 1, 2, 3 \tag{26}$$

where I_{Ti} is the total undeformed moment of inertia about the ith axis and is defined as

$$I_{Ti} = (I_i + 2\int_0^L (a+\xi)^2\rho_i A_i \, \mathrm{d}\xi) \qquad i = 1, 2 \tag{27}$$

and

$$I_{Ti} = (I_i + 4\int_0^L (a+\xi)^2\rho_i A_i \, \mathrm{d}\xi) \qquad \text{i} = 3 \tag{28}$$

The design requirements can be specified in terms of the natural frequency ω and damping ζ of the closed-loop system. The gains are calculated to satisfy the preceding requirements using the formulas given subsequently:

$$k_1 = 2I_{Ti}\omega^2 \tag{29}$$

$$k_2 = 2I_{Ti}\zeta\omega \tag{30}$$

The feedback law chosen leads to the following differential equation

$$I_{Ti}\dot{\omega}_i = -k_1\beta_{i_e} - k_2\omega_i \tag{31}$$

$$\Rightarrow I_{Ti}\ddot{\theta}_i = -k_1\frac{\theta_i}{2} - k_2\dot{\theta}_i \tag{32}$$

Simulation of the Lyapunov controller is presented in the penultimate section of this paper.

IV. Minimum-Time Control

The minimum-time control profiles for rest-to-rest maneuvers of a rigid body are bang-bang in nature. The number of switches and the switch times can be determined using a parameter optimization approach. The rigid-body equations of motion are given by

$$I\dot{\underline{\omega}} + \tilde{\underline{\omega}}I\underline{\omega} = \underline{U} \tag{33}$$

where I is the inertia matrix and $\tilde{\underline{\omega}}$ is the angular velocity cross product operator.

A parameter optimization problem is formulated[13] to minimize the cost function

$$\mathrm{J} = \tfrac{1}{2}p_0^2 \tag{34}$$

subject to

$$\dot{x} = f(x, U(p_i), t)p_0 \qquad t \in (0, 1) \tag{35}$$

$$x(1) = x_f, \; g(p_i) \geq 0 \qquad i = 1, \ldots, \mathrm{n} \tag{36}$$

where p_0 and p_i are $n + 1$ parameters to be selected, p_0 is the final time, and the rest of the parameters define the switch times and the maximum amplitude of the control effort. The function g defines the inequality constraints and $x(1)$ are the terminal boundary constraints. The bang-bang control is parameterized as

$$u = -p_1\mathrm{sgn}[(t-p_2)(t-p_3)] \tag{37}$$

for a control with two switches. The sensitivity of the final states to the individual parameters are obtained by finite differencing. In this work the parameters were solved for using sequential quadratic programming (SQP). It has been shown that for a spherical body, the number of switches can be either five or seven[15,16] based on the boundary conditions. The presence of the time-delay filter (Sec. V) can explicitly be incorporated into the optimization process. This way, the open-loop optimization takes the time delay into account.

V. Input Shaping and Time-Delay Control

Because present-day spacecraft are becoming increasingly lightweight and flexible, there is a growing need to design controllers that do not excite the vibratory modes of the system. In the problem of reorientation, the step input leads to the feedback controller "kicking" the system into motion due to the large initial error; this large control action can excessively excite the vibratory modes of the system. This is the motivating reason for modifying the reference input to attenuate vibration of the flexible appendages. A time-delay filter to achieve this objective is presented in the next section.

Time-delay controllers designed to cancel the poles of a system with the intention of attenuating the residual vibration has been shown to correspond to the two-impulse shaped-input controller[8] by Singh and Vadali.[14] It has further been shown that the three-impulse shaped-input controller (designed to increase robustness) is equivalent to using two time-delay controllers in series. The design of time-delay controllers to cancel the poles of the system is presented in this section.

Figure 3 illustrates a time-delay controlled second-order underdamped system. We need to determine A_0, A_1, and T so that the poles of the system are cancelled by the zeros of the controller, which are given by the equation

$$A_0 + A_1\exp(-sT) = 0 \tag{38}$$

A_0 is the amplitude of the proportional signal and T is the delay time of the time-delayed signal, which has a gain of A_1. Representing the Laplace variable s as

$$s = \sigma + j\omega \tag{39}$$

and substituting Eq. (39) into Eq. (38) and equating the real and imaginary parts to zeros, we have

$$A_0 + A_1\exp(-\sigma T)\cos(\omega T) = 0 \tag{40}$$

and

$$A_1\exp(-\sigma T)\sin(\omega T) = 0. \tag{41}$$

To ensure that the time-delay filter does not act as an amplifier or attenuator, we arrive at the third equation

$$A_0 + A_1 = 1 \tag{42}$$

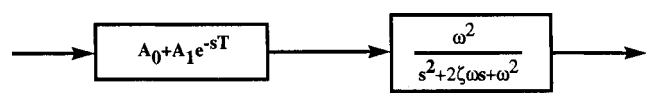

Fig. 3 Time-delay controlled system.

From Eq. (41) we have

$$\omega = (2n + 1)(\pi/T),\ 2n(\pi/T) \tag{43}$$

Substituting Eq. (43) into Eqs. (40) and (42), we have

$$A_0 = \frac{-\exp(-\sigma T)}{1-\exp(-\sigma T)} \tag{44}$$

and

$$A_1 = \frac{1}{1-\exp(-\sigma T)} \tag{45}$$

We see that only $\omega = (2n + 1)\pi/T$ produces positive values for A_0.

To cancel the system poles at $s = -\zeta_i\omega_i \pm j\omega_i\sqrt{1-\zeta_i^2}$, we have from Eq. (43) (setting $n = 0$)

$$\omega = \omega_i\sqrt{1-\zeta_i^2} = \pi/T \tag{46}$$

$$\Rightarrow T = \frac{\pi}{\omega_i\sqrt{1-\zeta_i^2}} \tag{47}$$

and

$$\sigma = -\zeta_i\omega_i \tag{48}$$

Substituting Eq. (48) into Eqs. (44) and (45), we have

$$A_0 = \frac{\exp(\zeta_i\pi/\sqrt{1-\zeta_i^2})}{1+\exp(\zeta_i\pi/\sqrt{1-\zeta_i^2})} \tag{49}$$

and

$$A_1 = \frac{1}{1+\exp(\zeta_i\pi/\sqrt{1-\zeta_i^2})} \tag{50}$$

This corresponds exactly to the solution of the shaped-input technique. The controller can also be written as

$$u(s) = (s^2 + 2\zeta_i\omega_i s + \omega_i^2)(s^2 + 2\zeta_i\omega_i s + 9\omega_i^2 - 8\zeta_i^2\omega_i^2)\ldots$$
$$(s^2 + 2\zeta_i\omega_i s + n^2\omega_i^2 - (n^2-1)\zeta_i^2\omega_i^2)R(s)$$
$$n = 1, 3, 5, \ldots \tag{51}$$

where $R(s)$ is the reference input and $u(s)$ is the filtered output. Thus the single time-delay controller can also be used to cancel poles of the system that are odd multiples of the two primary poles.

Singh and Vadali[14] have demonstrated the addition of robustness to the time-delay filter, to errors in estimated parameters of the system, by the multiple use of the single time-delay filter in cascade. Using multiple instances of this time-delay filter amounts to locating multiple zeros at the system pole location.

Although the equations of motion of the hub-appendage system are nonlinear, we use the robust time-delay filter to study its ability to deal with the nonlinear system. For the design of the time-delay controller for the hub-appendage system, the equations of motion are linearized about the final states, and the resulting eigenvalues are used in the design of the controller.

The eigenvalues of the Lyapunov-controlled system about the final attitude is required for the design of the time-delay controller. The feedback gains are selected so that the controller produces an underdamped response with a period of 50 s and a 5% settling time of 100 s. This leads to a damping ratio of 0.3 and a natural frequency of 0.133 rad/s. This has been done deliberately to illustrate the attenuation of vibrations of two frequencies simultaneously. The feedback gains chosen to meet the requirements are

$$k_1 = 68.51 \quad \text{and} \quad k_2 = 154.53 \tag{52}$$

These gains were arrived at considering the linearized equation corresponding to motion about the X axis. These gains lead to a different natural frequency and damping ratio for motion about the z axis. We use this difference in frequency to illustrate the ability of the time-delay filter to handle variations in frequency.

The eigenvalues of the closed-loop linearized system (18th order) about the final states are

(1) $-0.0235 \pm 0.1014j$; (2) $-0.0368 \pm 0.1257j$

(2) $-0.0381 \pm 0.5875j$; (1) $-0.0376 \pm 0.6686j$

(2) $-0.0018 \pm 2.7169j$; (1) $-0.0026 \pm 2.7386j$

The numbers in parentheses indicate the multiplicity of the eigenvalues.

The time-delay filter to cancel the poles at $-0.0381 \pm 0.5875j$; and attenuate the poles at $-0.0376 \pm 0.6686j$ has a transfer function

$$\frac{u(s)}{R(s)} = 0.0710 + 0.2662e^{-5.3464s} + 0.3742e^{-2*5.3464s} + 0.2338e^{-3*5.3464s} + 0.0548e^{-4*5.3464s}$$

The filter is designed based only on the poles at $-0.0381 \pm 0.5875j$. To design a better filter, we would have to design filters for each of the pairs of poles and use them in cascade. We use the robust version of the filter to illustrate the control of frequencies in the vicinity of the design frequency. The robust filter consists of four single time-delay filters in cascade.

The time-delay filter to cancel the poles at $-0.0235 \pm 0.1014j$ and to attenuate the effect of poles at $-0.0368 \pm 0.1257j$ has a transfer function

$$\frac{u(s)}{R(s)} = 0.3110 + 0.4933e^{-30.98s} + 0.1956e^{-2*30.98s}$$

The modified reference input to eliminate the frequencies $-0.0235 \pm 0.1014j$ and $-0.0368 \pm 0.1257j$ and others in their vicinity, when the plant is subject to a unit step input, is arrived at by filtering the step input through the time-delay filters designed for each of these frequencies.

The results of the Lyapunov controller used in conjunction with the time-delay filter are presented in the next section.

VI. Simulation

The proposed controllers are tested on the reorientation problem of a hub-appendage system. The initial attitude for all the simulated controllers corresponds to the coincidence of the body axis frame to the inertial frame. The final attitude corresponds to the Euler parameter set

$$\begin{Bmatrix}\beta_0\\ \beta_1\\ \beta_2\\ \beta_3\end{Bmatrix} = \begin{Bmatrix}0.6633\\ 0.2\\ 0.4\\ 0.6\end{Bmatrix} \tag{53}$$

The flexible spacecraft parameters are

$$\rho A = 0.0004 \text{ kg/m}, \qquad a = 1.0 \text{ m}$$

$$EZ = 1500 \text{ N m}^2, \qquad L = 151 \text{ m}$$

$$I_{Tx} = 1936.5 \text{ kg m}^2, \qquad I_{Ty} = 1936.5 \text{ kg m}^2$$

$$I_{Tz} = 3073.0 \text{ kg m}^2$$

This leads to an inertia ratio of the flexible to the rigid portion of the structure to be

$$I_f/I_r = 936.5/1000 \tag{54}$$

for the X and y axis and

$$I_f/I_r = 1873/1200 \tag{55}$$

for the z axis, where I_f and I_r are the moment of inertia of the flexible and rigid portions of the spacecraft about the slew axis, respectively. The first simulation consists of control of the spacecraft using the Lyapunov controller. The graph of the Euler parameters reveals an underdamped motion leading to overshoot of the Euler parameters (Fig. 4a). The slew and settling time of the rigid body is more than 100 s. Figure 5a illustrates the motion of the tip of one of the flexible appendages. The analogy of the single-link flexible-arm robot can be used to explain the initial motion of the flexible appendage. The nonminimum phase characteristic of the flexible-arm robot results in the flexible link moving in the direction opposite the desired direction of motion.[17] The large

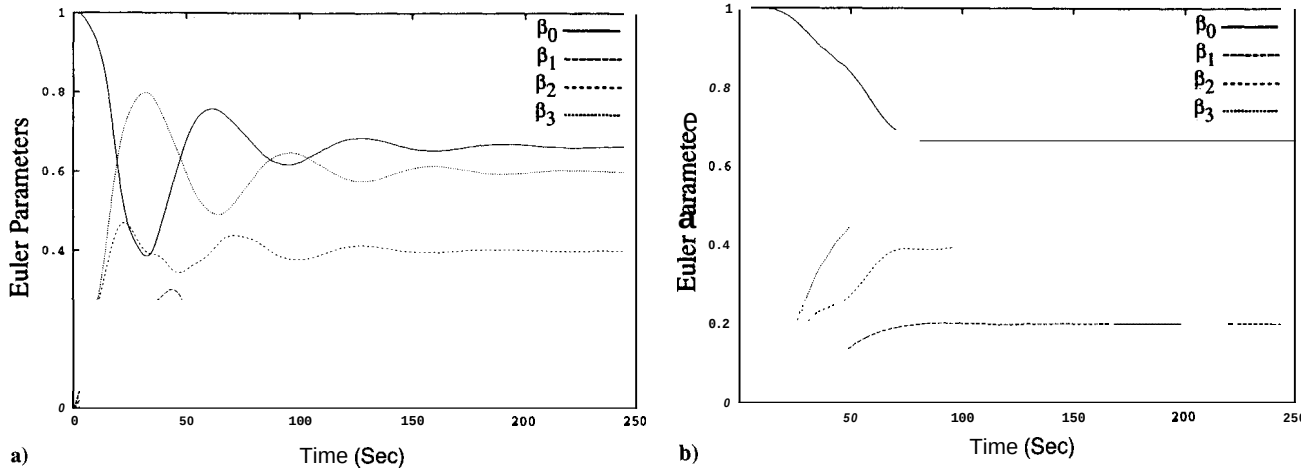

Fig. 4 Time history of Euler parameters: a) Lyapunov control and b) Lyapunov/time-delay control (15-time-delays).

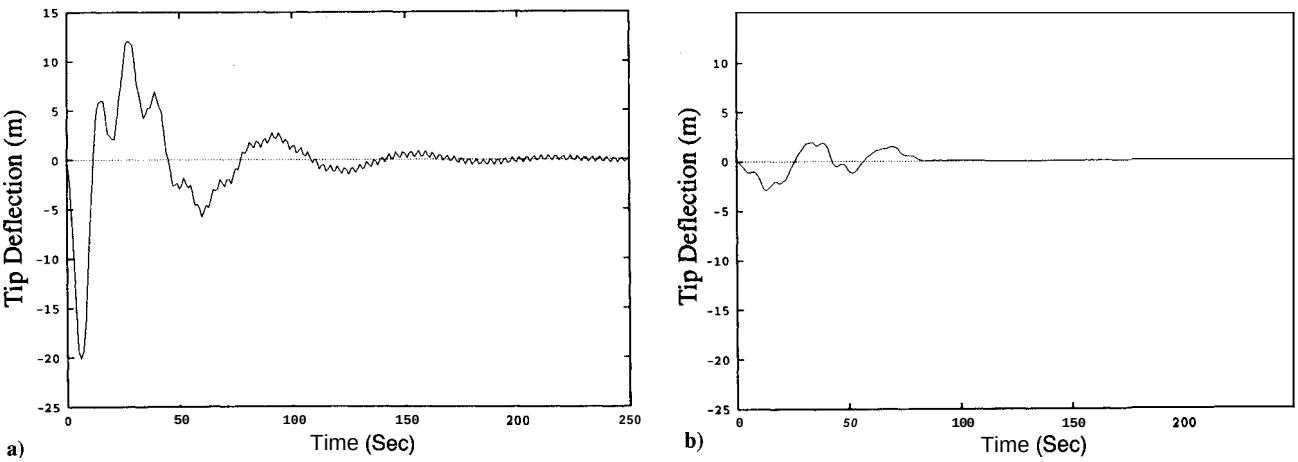

Fig. 5 Tip deflection of appendage: a) Lyapunov control and b) Lyapunov/time-delay control (15-time-delays).

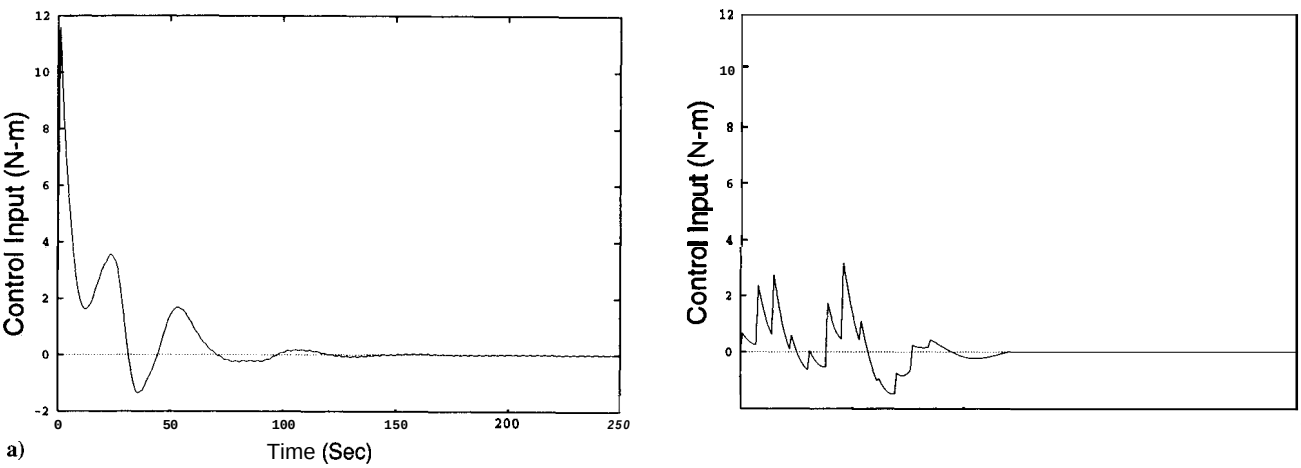

Fig. 6 Control torque history: a) Lyapunov control and b) Lyapunov/time-delay control (15-time-delays).

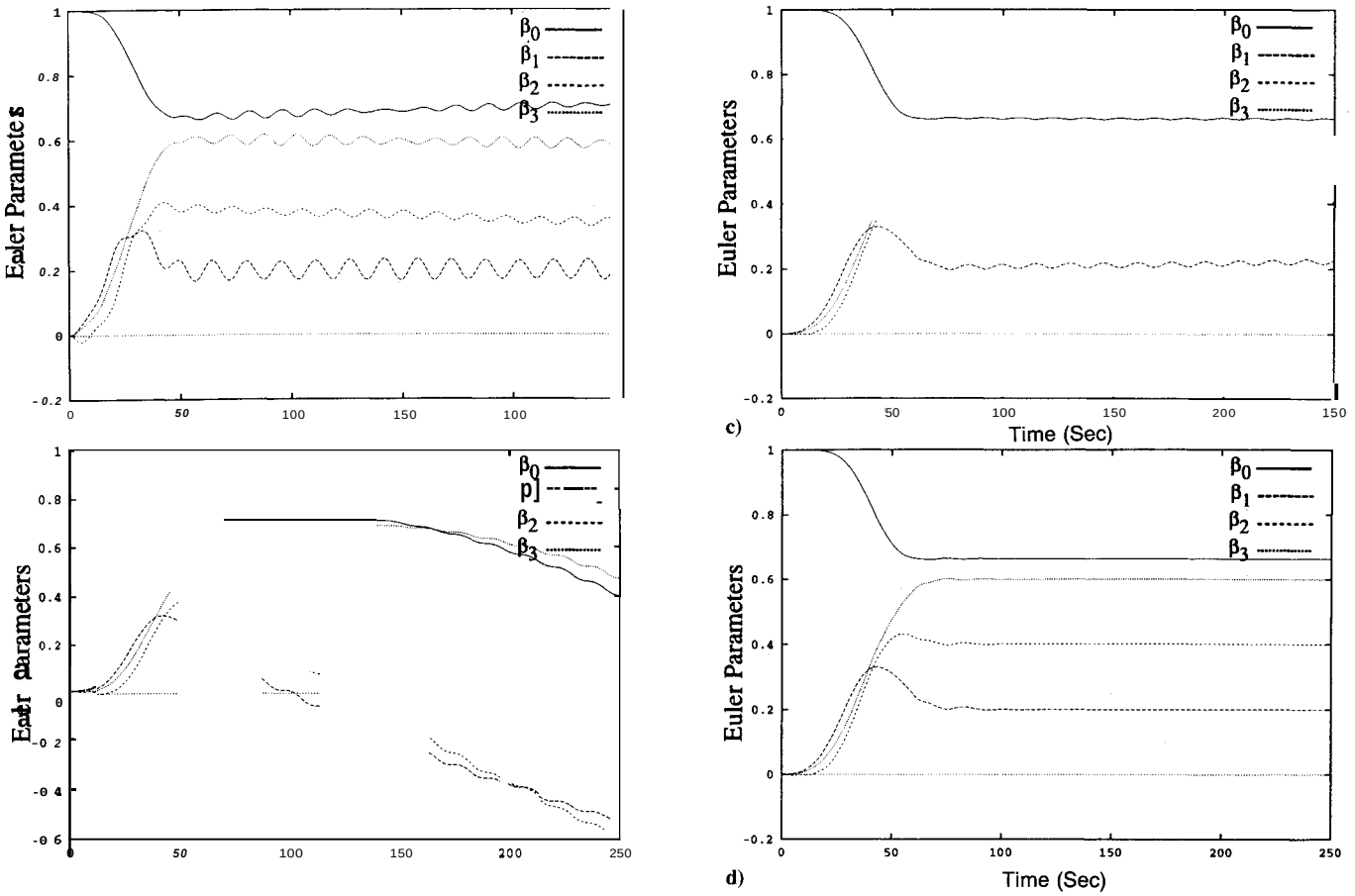

Fig. 7 Time history of Euler parameters: a) time-delay shaped bang-bang control, b) post time-delay filtered bang-bang control, c) time-delay filtered bang-bang control, and d) time-delay filtered bang-bang control with end game feedback control.

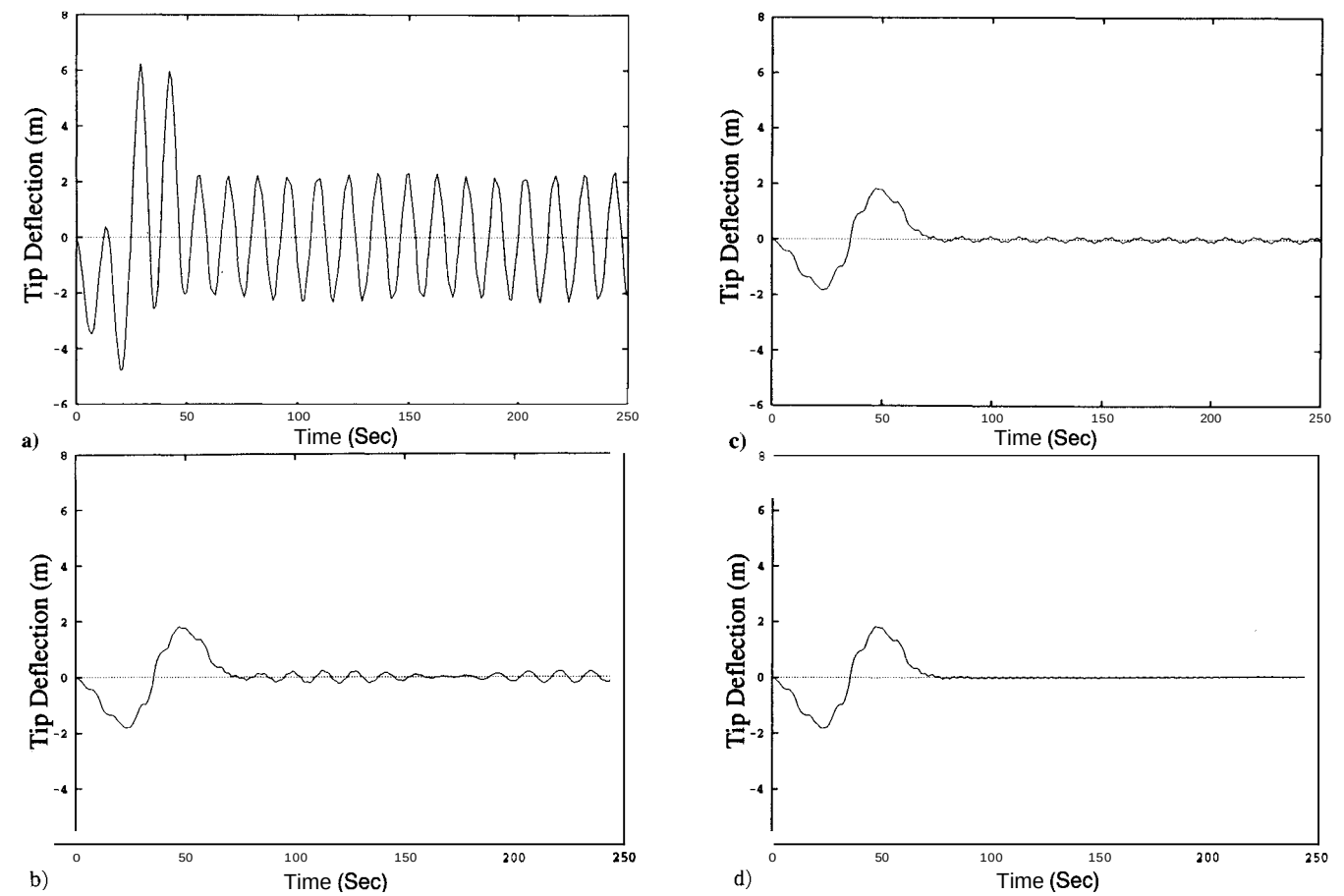

Fig. 8 Tip deflection of appendage: a) time-delay hang-bang control, b) post time-delay filtered bang-bang control, c) time-delay filtered bang-bang control, and d) time-delay filtered bang-bang control with end game feedback control.

displacement of the tip is asymptotically forced to zero by the Lyapunov controller. Figure 6a, which shows the control input of one of the actuators, exemplifies the spike in the control action required due to the large initial error in the attitude. The effect of the vibratory motion of the flexible link contributes to the oscillation in the control input in spite of the controller being a function of the angular velocity and the attitude because the rigid-body mode and the flexible modes are coupled.

The second simulation involves elimination or reduction in the overshoot of the rigid-body motion. The filter for the elimination of the frequency corresponding to the rigid-body motion is used in cascade with the time delay filter designed to attenuate the contributions of the first mode of vibration of the appendages. This filter with 15 time delays seems to provide a very elegant technique to reorient the spacecraft. Figure 4b illustrates the significant reduction in the overshoot of the rigid-body motion compared with the overshoot when the Lyapunov controller was used. The tip motion of the appendage reveals a motion that is insignificant compared to the first controller (Fig. 5b). Finally, Fig. **6b** helps to verify that a smaller peak torque is required.

The next set of simulations exemplifies the fact that the time-delay filter can be used to reduce the vibratory motion of the structure even in an open-loop setting. **A** 5 N-m bound was selected for each of the actuators and the optimization program converged to a five-switch bang-bang profile for the rigid-body model. The first simulation involves the hub-appendage system being subject to a time-optimal bang-bang controller. Figure 7a illustrates the evolution of the Euler parameters. It can be seen that the application of the bang-bang control profile, designed based on the rigid-body model, does not meet the boundary conditions of the system that includes the flexible-body modes. In addition it also excites the flexible appendage, the effect of which on the Euler parameters is revealed by the oscillations present after the bang-bang control is complete. Figure 8a demonstrates the large residual vibration of the tip of the first appendage in the y direction. Figure 9a represents the five-switch bang-bang control profile.

The next simulation illustrates that the time-delay filter cannot be used directly to modify the bang-bang input after the bang-bang control profile has been designed. Figure 7b represents the evolution of the Euler parameters when the time-optimal control profile is filtered through a time-delay filter designed to eliminate the first mode of vibration of the appendage. Because the time-delay filter is based on linear theory, there is considerable residual velocity, which leads to the Euler parameters drifting after the control torque is zero (Fig. 9b). Figure 8b, however, reveals that the time-delay filtering reduced the vibration of the tip of the appendage significantly.

To reduce residual vibration via the time-delay filter, the time-delay filter is concatenated to the plant and the bang-bang control profile is designed for this modified plant. Figure 7c reveals that this procedure works very well, leading to the Euler parameters reaching the desired position with small error in residual velocity and vibration. The objective of using the time-delay filter is achieved (Fig. 8c) by the small amplitude of vibration of the tip of the appendage. Figure 9c reveals that the control profile is different from the previous case (Fig. 9b).

The final simulation involves the use of an end-game controller. **A** Lyapunov-based feedback controller designed to produce a natural frequency of 0.133 rad/s and a damping of 0.8 is gradually included into the system at the end of the bang-bang control profile. **A** multiplier function $(\tau^2(3 - \mathbf{27}))$ gradually introduces the effect of the Lyapunov controller, where τ is the time referenced from the instant when the Lyapunov controller was introduced. Figure 7d illustrates that the small residual errors present at the end of the previous

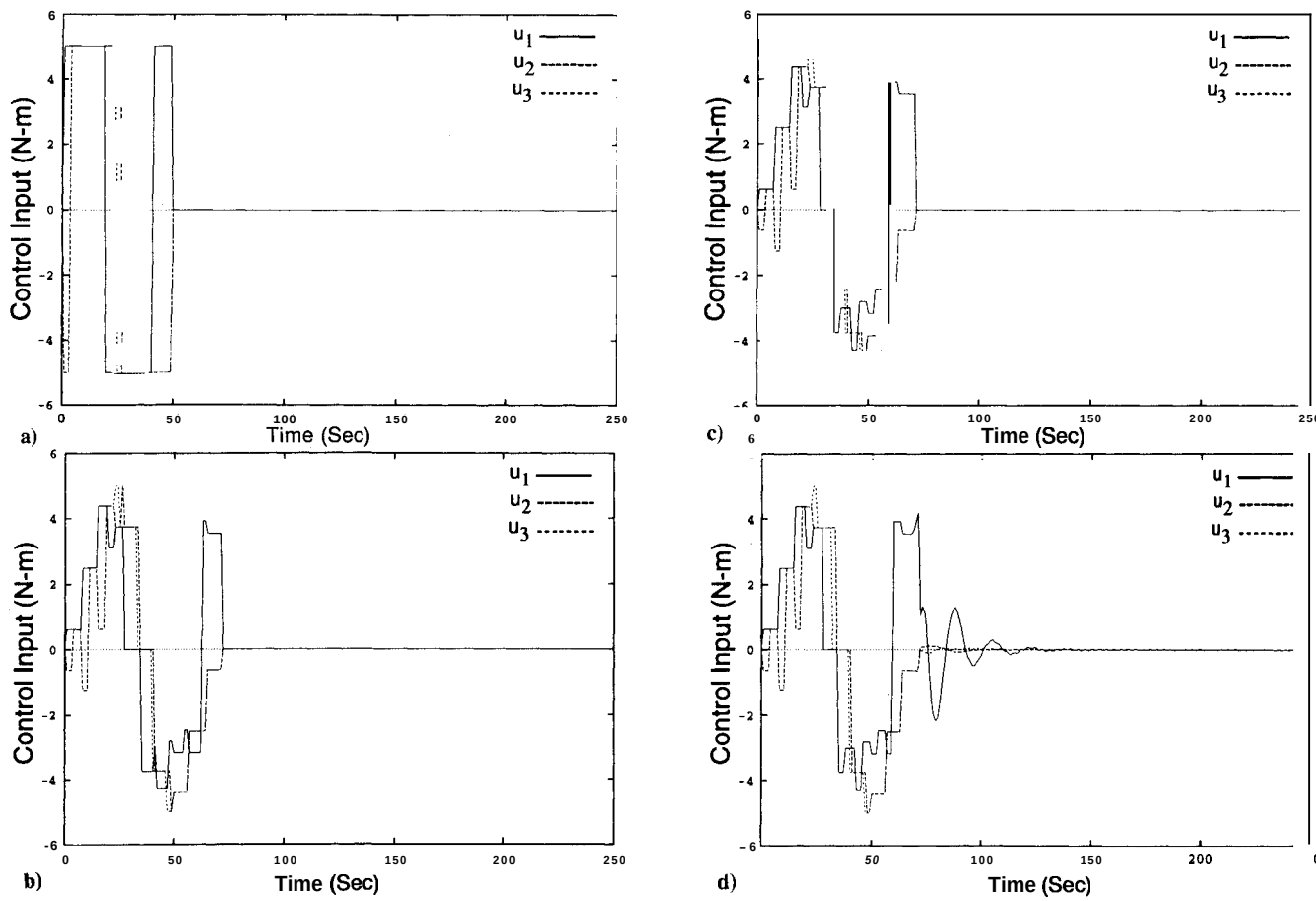

Fig. 9 Control torque history: a) time-delay bang-bang control, b) post time-delay filtered bang-bang control, c) time-delay filtered bang-bang control, and d) time-delay filtered bang-bang control with end game feedback control.

simulation are eliminated. The tip vibration (Fig. 8d) is essentially the same as in the previous case. It can be seen in Fig. 9d that the control profile is essentially the same as that in Fig. 9c for 70 s, which is when the Lyapunov controller is introduced to control the system.

VII. Conclusions

An elegant control strategy has been proposed combining the robustness of the Lyapunov controller to modeling errors and the robustness of the time-delay controller to estimated frequency and damping. The stability proof of the Lyapunov controller does not at any time consider the model of the system being controlled. A good estimate of the inertia of the system is, however, useful to help select gains for a desired performance. In the same vein, the design of the time-delay controller for a nonlinear system based on its linearized model is a powerful approach, as seen from the excellent results shown in the paper.

It is observed that when the open-loop controller is designed with the time-delay controller in place, the results are truly remarkable.

Acknowledgments

This research was performed under the NASA-Air Force control-structure-interaction guest investigator program (contract NASI-19373). The authors gratefully acknowledge helpful discussions and comments provided by Alok Das and Derek Cossey of the Air Force Phillips Laboratory, Edwards Air Force Base, California. Suggestions by John L. Junkins are appreciated.

References

[1]Vadali, S. R., "Feedback Control of Space Structures: A Liapunov Approach," *Mechanics and Control of Large Flexible Structures*, edited by J. L. Junkins, Vol. 129, Progress in Astronautics and Aeronautics, AIAA, Washington, DC, 1990, Chap. 24.

[2]Fujii, H., Ohtsuka, T., and Udou, S., "Mission Function Control for a Slew Maneuver Experiment," *Journal of Guidance, Control, and Dynamics*, Vol. 14, No. 5, 1991, pp. 986–992.

[3]Junkins, J. L., Rahman, Z., and Bang, H., "Near-Minimum Time Maneuvers of Flexible Vehicles: A Liapunov Control Law Design Method," *Mechanics and Control of Large Flexible Structures*, edited by J. L. Junkins, Vol. 129, Progress in Astronautics and Aeronautics, AIAA, Washington, DC, 1990, Chap. 22.

[4]Singh, T., Golnaraghi, M. F., and Dubey, R. N., "Sliding-mode/Shaped-input Control of Flexible/Rigid Link Robots," *Journal of Sound and Vibration*, Vol. 166, No. 3, 1993.

[5]Hablani, B. H., "Zero-Residual-Energy, Single-Axis Slew of Flexible Spacecraft with Damping, Using Thrusters: A Dynamic Approach," *Proceedings of the AIAA Guidance, Navigation, and Control Conference* (New Orleans, LA), Vol. 1, AIAA, Washington, DC, 1991, pp. 488–500.

[6]Skaar, S. B., Tang, L., and Yalda-Mooshabad, I., "On-Off Attitude Control of Flexible Satellites," *Proceedings of the AIAA Guidance, Control, and Navigation Conference* (Monterey, CA), Vol. 2, AIAA, New York, 1986, pp. 1222–1228.

[7]Smith, O. J. M., *Feedback Control Systems*, McGraw-Hill, New York, 1958.

[8]Singer, N. C., and Seering, W. P., "Preshaping Command Inputs to Reduce System Vibrations," *ASME Journal of Dynamic Systems, Measurement, and Control*, Vol. 112, March 1990, pp. 76–82.

[9]Wie, B., and Liu, Q., "Feedforward/Feedback Control Synthesis for Performance and Robustness," *Proceedings of the AIAA Guidance, Navigation, and Control Conference* (Portland, OR), AIAA, Washington, DC, 1990, pp. 996–1005.

[10]Junkins, J. L., and Turner, J. D., *Optimal Spacecraft Rotational Maneuvers*, Elsevier, Amsterdam, 1986, p. 335.

[11]Wie, B., Weiss, H., and Arapostathis, A., "A Quaternion Feedback Regulator for Spacecraft Eigenaxis Rotations," *Journal of Guidance, Control, and Dynamics*, Vol. 12, No. 3, 1989, pp. 211–235.

[12]Oh, H. S., Vadali, S. R., and Junkins, J. L., "Use of the Work-Energy Rate Principle for Designing Feedback Control Laws," *Journal of Guidance, Control, and Dynamics*, Vol. 15, No. 1, 1992, pp. 275–277.

[13]Vadali, S. R., Singh, T., and Carter, T., "Computation of Near-Minimum-Time Maneuvers of Flexible Structures by Parameter Optimization," *Proceedings of the AIAA Guidance, Navigation, and Control Conference* (Hilton Head, SC), Vol. 2, AIAA, Washington, DC, 1992, pp. 694–704.

[14]Singh, T., and Vadali, S. R., "Robust Time-Delay Control," *ASME Journal of Dynamic Systems, Measurement, and Control*, Vol. 115, No. 2(A), 1993, pp. 303–306.

[15]Bilimoria, K. D., and Wie, B., "Minimum Time Large Angle Reorientation of a Rigid Spacecraft," AIAA Guidance, Navigation, and Control Conf., AIAA Paper 90-3486, Portland, OR, Aug. 1990.

[16]Byers, R. M., and Vadali, S. R., "A Quasi Closed Form Solution to the Time Optimal Rigid Body Reorientation Problem," First AAS/AIAA Spacecraft Mechanics Conf., AAS 91-124, Johnson Space Center, Houston, TX, Feb. 11–13, 1991.

[17]Vidyasagar, M., "On Undershoot and Nonminimum Phase Zeros," *IEEE Transactions on Automatic Control*, Vol. **AC-31,** No. 5, 1986, p. 440.